20th Australasian Fluid Mechanics Conference
Perth, Australia
5-8 December 2016

Development of a Cavitation Susceptibility Meter for Nuclei Size Distribution Measurements

M. T. Khoo[1], J. A. Venning[2], B. W. Pearce[2], P. A. Brandner[2] and Y. Lecoffre[3]

[1]Defence Science and Technology Group, Fishermans Bend, Victoria, 3207, Australia
[2]Australian Maritime College, University of Tasmania, Launceston, Tasmania, 7250, Australia
[3]Hydeo France, Grenoble, 38000, France

Abstract

Cavitation inception in practical flows is invariably heterogeneous as nucleation sites are provided by microbubble populations. Microbubbles grow explosively, filling with vapour, when exposed to a critical pressure which is size dependent. The detection of physical bubble activations in a known pressure field can therefore be used to measure bubble size distributions. The nuclei population within a test flow can be measured using a venturi and by counting the number of activations or events using the acoustic emission from each bubble collapse in the downstream pressure recovery region. Such devices are known as Cavitation Susceptibility Meters (CSMs).

The development, calibration and operation of a CSM for use in the cavitation tunnel at the Australian Maritime College is described. The minimum pressure in the CSM is reduced in steps by increasing the flow rate or decreasing tunnel static pressure to activate increasing numbers of smaller nuclei in order to provide a cumulative size distribution. Simultaneous flow rate measurement permits nuclei volumetric concentration as well as venturi throat pressure to be determined.

The concentration measurement is shown to have an uncertainty of less than 0.5%, while the critical pressure has an uncertainty of approximately 5%. The volume measurement and timing uncertainties for flow rate calibration are found to account for 81% of this uncertainty. Sample nuclei distribution measurements are presented, showing critical pressures as low as 100 kPa below vapour pressure, corresponding to an equivalent bubble diameter of 1 μm in the test section.

Introduction

The presence of microbubbles, or nuclei, in water is known to control the inception and dynamic behaviour of cavitation about marine propulsors [1, 8, 15]. The equilibrium of a microbubble at external pressures below a critical value becomes unstable such that it will grow explosively. By this mechanism, they provide heterogeneous cavitation nucleation sites. The dynamic behaviour of microbubbles is described by the Rayleigh-Plesset equation [7]. Knowledge of nuclei content in cavitation tunnel water is essential to accurately assess the cavitation performance of test components.

Optical and hydrodynamic techniques are generally used to measure nuclei distributions in water. Optical techniques include holography [11], Interferometric Laser Imaging [11], shadowgraphy [14, 17] and Phase Doppler Analysis [8]. These techniques enable direct measurements of nuclei size and concentration. However, they may falsely identify contaminant particles as microbubbles and have a minimum detectable size due to optical diffraction limits. Depending on the implementation, these methods possess varying degrees of temporal and spatial resolution. A Cavitation Susceptibility Meter (CSM) is a hydrodynamic device that uses a venturi to induce cavitation inception and therefore measure the critical pressure of microbubbles and other active nuclei. It allows nuclei smaller than 1 μm in diameter to be measured. Bubble size can be derived from the measured critical pressure using the equations for a bubble in equilibrium [7]. As the test flow must be sampled, this method lacks spatial and temporal resolution and is effective for flows with homogeneous nuclei distributions. It has been used in laboratory [4, 6, 9, 11, 12, 13] and real-world environments [16].

A CSM developed by YLec Consultants, also known as the 'Venturix' [13], was implemented to measure the nuclei size distribution in the water tunnel at the Australian Maritime College's Cavitation Research Laboratory. The variable-pressure, closed-circuit cavitation tunnel has a volume of 365 m^3 (demineralised water). The test section has a 0.6×0.6 m cross section and is 2.6 m long. It has ancilliaries for fast degassing and nuclei injection that enable strict control of the nuclei content. A schematic of the tunnel is shown in figure 1. Further details regarding the tunnel design and operation are described in [2].

Implementation of both a CSM and a nuclei injection system enables rigorous experimental modelling of cavitation inception and dynamic behaviour of marine propulsors to be conducted.

CSM Design and Operating Principle

Water is continuously sampled from the tunnel test section and passed through a contraction, or throat, in the venturi which is formed by the annular gap between a centrebody and an external sleeve (figure 2). This design is simpler to manufacture than conventional venturis and allows alternate external sleeves to be fitted for various diagnostics (eg. imaging and pressure characterisation). Boundary layer tripping devices are used to generate turbulent flow around the centrebody, thus delaying boundary layer separation in the downstream diffuser which gives rise to undesirable sheet cavitation.

As the tunnel static pressure is reduced or dynamic pressure in the venturi throat increased, the throat static pressure (p_{VT}) reduces below vapour pressure (p_v). Larger free gas bubbles (in the order of 100 μm) collapse at or above this pressure. However, smaller nuclei sustain larger negative pressures prior to reaching their critical pressure (p_c), at which point they become unstable and grow explosively. With the onset of cavitation, the minimum venturi throat pressure is equal to the critical pressure of the smallest nuclei being activated. Using the formulas for spherical bubble equilibrium [7], the following polynomial is derived, which is solved numerically to give the equivalent initial bubble diameter (D_0),

$$\frac{4}{27\left(p_v-p_c\right)^2}=\left(\frac{D_0}{4S}\right)^3\left(p_0-p_v\right)+\left(\frac{D_0}{4S}\right)^2 \qquad (1)$$

where S is the surface tension and p_0 is the initial pressure.

Once nuclei are activated and grow in the venturi throat, they are advected downstream into a high pressure region in the diffuser where they collapse. The collapse of the vapour-filled bubble generates a shockwave, the propagation of which excites a structural response in the venturi outer sleeve that is measured by a piezoceramic sensor. Each event is counted using signal

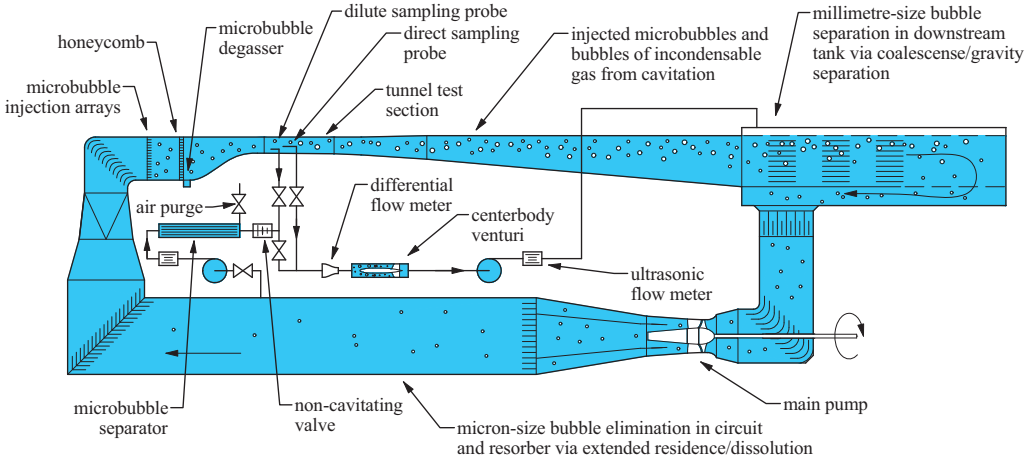

Figure 1: Schematic of the cavitation tunnel and CSM circuit.

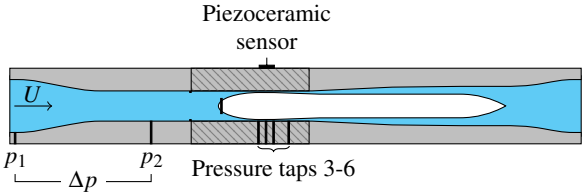

Figure 2: Schematic showing venturi arrangement, including the interchangable outer sleeve (shaded area) with pressure taps and piezoceramic sensor.

processing. The nuclei event rate and concentration (C) is then calculated for the sampled water by,

$$C = \frac{N}{\Delta t Q} \tag{2}$$

where N is the number of activations counted over time Δt, and Q is the volumetric flow rate. The critical pressures of the activated nuclei are determined using the minimum pressure coefficient in the venturi throat which is measured under non-cavitating conditions. Direct measurement of the minimum throat pressure in real time is not possible due to destabilisation of the pressure field during cavitation events and undesirable cavitation at the pressure taps.

Differential Flow Meter Calibration

The volumetric flow rate can be measured using ultrasonic flow meters, although for redundancy and field use, a differential flow meter can be useful. In this case, the volumetric flow rate is determined using the measured differential pressure, $\Delta p = p_1 - p_2$, across a contraction located upstream of the centrebody venturi. The Bernoulli equation for incompressible flow across the contraction is modified to incorporate a flow coefficient (C_Q) which characterises the viscous losses and geometric parameters of the contraction. The flow coefficient is given by,

$$C_Q = \frac{Q}{A_2\sqrt{2\Delta p/\rho}} \tag{3}$$

where A_2 is the contraction outlet area and ρ is fluid density. C_Q was determined from calibration. A differential pressure sensor (Siemens P500, span: 0–31.25 kPa, model: 7MF5403-1EA10-Z) was used to measure the contraction pressure difference while tunnel water was pumped through it and collected in a tank. The flow rate was calculated by dividing the measured volume by the water discharge time. The flow coefficient was measured for a range of Reynolds numbers based on the contraction outlet diameter. A power law trendline was fitted to the data,

$$C_Q = a_1 \times Re^{b_1} \tag{4}$$

where $a_1 = 0.826$ and $b_1 = 0.0186$. The Reynolds number is defined as $Re = U_2 D_2/\nu$, where U_2 is the mean flow velocity at the outlet of the contraction, D_2 is the contraction outlet diameter and ν is the fluid kinematic viscosity. The measured C_Q data and corresponding trendline are shown in figure 3.

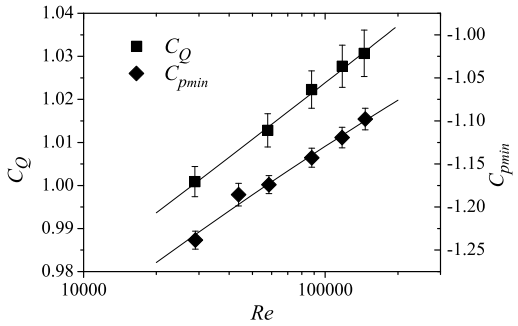

Figure 3: Flow coefficient (C_Q) for the contraction and minimum pressure coefficient ($C_{p_{min}}$) in the venturi throat as functions of Reynolds number.

The flow velocity at the outlet of the contraction, U_2, is then,

$$U_2 = \left[a_1 \left(\frac{D_2}{\nu} \right)^{b_1} \left(\frac{2\Delta p}{\rho} \right)^{0.5} \right]^{\frac{1}{1-b_1}} \tag{5}$$

This allows the volumetric flow rate to be determined, then used in equation 2 to calculate the nuclei concentration. The flow velocity is also used together with the venturi throat calibration parameters to determine the venturi throat pressure.

Venturi Throat Calibration

In order to determine the minimum throat pressure, the pressure coefficient (C_p) along the throat was measured as a function of Re under non-cavitating conditions. A sleeve with pressure taps at four locations along the venturi throat and pre-diffuser was installed (figure 2). Two of the upstream locations each had two opposing taps (not shown), allowing the alignment of

the centrebody within the sleeve to be assessed. The pressure coefficient at each pressure tap is defined as,

$$C_p = \frac{p_x - p_1}{\frac{1}{2}\rho U_{VT}^2} \tag{6}$$

where p_x is the pressure at location x in the throat, p_1 is the pressure at a reference location upstream of the venturi measured using high and low range absolute pressure sensors (Siemens DSIII, span: 0–500 kPa, model: 7MF4333-1GA02-2AB1 and Siemens DSIII, span: 0–130 kPa, model: 7MF4333-1FA02-2AB1, respectively) and U_{VT} is the mean flow velocity in the venturi throat, determined using either the ultrasonic flow meters (as shown in this paper), or the differential flow meter. Both methods were calibrated simultaneously. The streamwise variation of C_p is shown in figure 4 for a range of Re.

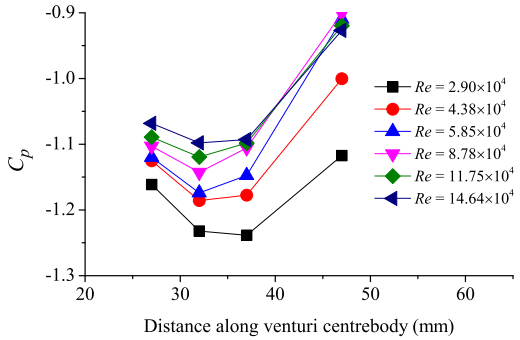

Figure 4: Variation of pressure coefficient along venturi centrebody for a range of Reynolds numbers. The throat is located between 27 and 37 mm. A pressure tap located downstream of the throat at 47 mm was also used.

The magnitude of C_p in the venturi throat decreases with increasing Re value. The minimum pressure coefficient ($C_{p_{min}}$) occurs at one streamwise location for all but the lowest Re value. Due to boundary layer growth, the location of the minimum pressure is downstream of the minimum geometrical throat area for all Re. A power law trendline was fitted to the $C_{p_{min}}$ values as a function of Re to give,

$$C_{p_{min}} = a_2 \times Re^{b_2} \tag{7}$$

where $a_2 = -2.53$ and $b_2 = -0.0701$. The measured $C_{p_{min}}$ data and corresponding trendline are shown in figure 3. The minimum venturi throat pressure (p_{min}) is determined from,

$$p_{min} = p_1 + \frac{1}{2}\rho a_2 \left(\frac{D_2}{\nu}\right)^{b_2} \left(\frac{A_2}{A_{VT}}\right)^2 U_2^{(b_2+2)} \tag{8}$$

This corresponds to the critical pressure (p_c) of the smallest activated nuclei.

Signal Processing Technique

Cavitation bubble collapse events are counted using the measured voltag (V_P) across a piezoceramic sensor (STEMiNC, 1 MHz resonant frequency, model: SMD15T21R111WL). The signal is measured at a sampling frequency of 2 MHz. Four stages of signal processing are used to shape each bubble collapse signal into an individual peak:

1. High-pass filter (to remove low frequency structural resonance and shorten event duration)
2. Rectification (to enable smoothing of data)
3. Low-pass filter (to smooth data into single peaks)
4. Log function (to homogenise nuclei event signal amplitudes, improving the effectiveness of peak counting)

Peak counting is used to count the number of maxima in the processed signal above a threshold level. The nuclei event and volumetric flow rates are used to calculate the nuclei concentration as per equation 2. Samples of the raw and processed signal from the piezoceramic sensor are provided in figure 5. The effect of the threshold level on the total nuclei count (for the complete dataset from which figure 5 data was extracted) is provided in figure 6. If the threshold is set too high, nuclei events are missed. Conversely, if the threshold level is set too low, additional peaks due to unfiltered structural resonance are counted, resulting in a higher nuclei concentration. The threshold level is currently set based on correlation of aurally-detected events and signal peaks. Further investigation of the acoustic emissions from bubble collapses is required to quantify the counting accuracy and to improve its performance.

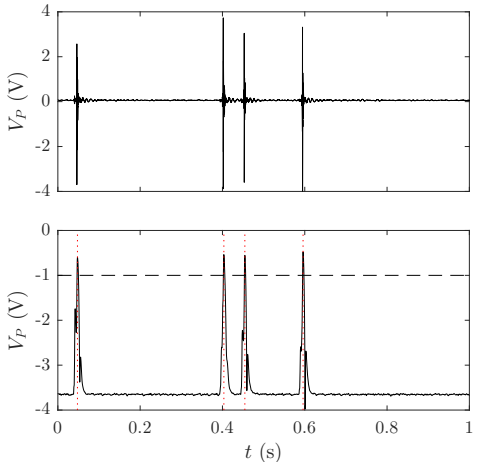

Figure 5: Piezoceramic sensor signal: raw (top) and processed (bottom). A threshold level of -1 (horizontal, dashed line) gives a count of 4. Vertical, dotted lines indicate detections.

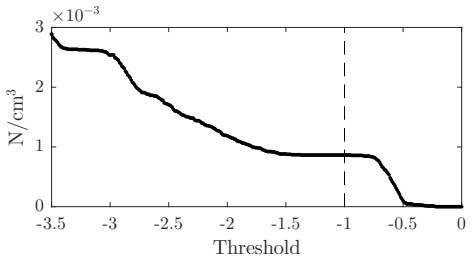

Figure 6: Effect of threshold setting on nuclei concentration.

Nuclei Distribution Measurement

A cumulative background nuclei distribution for the cavitation tunnel is shown in figure 7. Nuclei concentrations were measured at a range of throat pressures by increasing the venturi flow rate. The measurement method is cumulative, with a larger number of cavitation events occurring with decreasing pressure as all nuclei with a critical pressure greater than or equal to the throat pressure are activated. The results show that a nucleus with an equivalent bubble diameter in the test section less than 1.78 μm can sustain a pressure in the venturi throat of 49.1 kPa below vapour pressure before activation while a nucleus with an equivalent diameter less than 1.01 μm can sustain -95.2 kPa. The measured background nuclei concentrations in the order of 10^{-4} N/cm^3 are relatively low compared to the maximum anticipated concentrations in the laboratory environments in the

order of 10 N/cm^3. Nuclei generators can be used to control the concentration of artificially-seeded nuclei in the test section [3, 10].

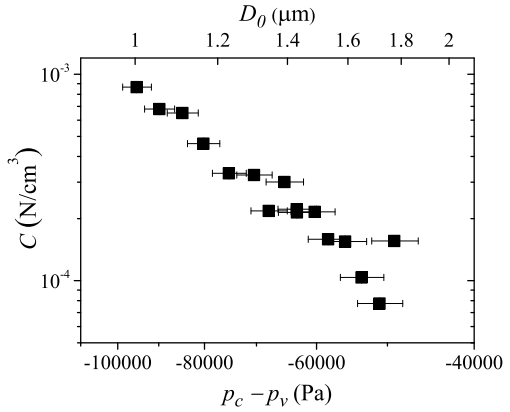

Figure 7: Cavitation tunnel cumulative background nuclei distribution. D_0 is the equivalent bubble diameter in the test section with static pressure 105 kPa and dissolved O_2 content 3 mg/L.

Uncertainty Analysis

An uncertainty analysis summary is provided in table 1. Bias errors were propagated for each of the measured quantities used to calculate the variables of interest, as described in [5]. For the nuclei concentration, the uncertainty in the activation count was assumed to be zero as validation of the event counting method has not been carried out. Further investigation of acoustic emissions from bubble collapses is required to quantify the counting accuracy. This will directly influence the nuclei concentration uncertainty. The main sources of uncertainty in the venturi throat pressure measurement were the C_p and U_2 measurements, both of which stem from the uncertainties in the tank volume and timing measurements. These two parameters account for 81% of the $p_c - p_v$ uncertainty, implying that it could be reduced with a more accurate direct flow rate calibration.

f	Ref. value	$\%\varepsilon_f$	Major contributors
C_Q	1.02	0.424	*Vol* (64%), Δt (35%)
U_2	4.21 m/s	0.435	C_Q (99%)
Q_{UT}	0.00123 m^3/s	0.465	*Vol* (53%), Δt (29%)
C_p	−1.14	0.970	Q_{UT} (92%)
Re	8.79×10^4	1.19	ν (85%), Q_{UT} (15%)
p_{VT}	−60,600 Pa	5.12	C_p (54%), U_2 (41%)
$C^\dagger$	0.000271 N/cm^3	0.436	U_2 (100%)
$p_c - p_v$	−63,100 Pa	4.92	C_p (54%), U_2 (41%)

Table 1: Uncertainties for a flow rate of 1.2 l/s at 25°C. ε_f is the total uncertainty in f, the variable of interest and *Vol* is the tank volume for flow meter calibration. † denotes that the error in activation count, N, was assumed to be zero.

Conclusions

The calibration and operation of a Cavitation Susceptibility Meter for use in the cavitation tunnel at the Australian Maritime College was presented. The flow and minimum pressure coefficients were calibrated experimentally for a range of Reynolds numbers. The sensitivity of the nuclei concentration measurement to threshold level setting was illustrated, highlighting the requirement for further investigation of acoustic emissions from bubble collapses to quantify the counting accuracy. The concentration measurement was shown to have an uncertainty of less than 0.5%, while the critical pressure had an uncertainty of approximately 5%. The volume measurement and timing uncertainties for flow rate calibration accounted for 81% of this uncertainty. Sample nuclei distribution measurements showed nuclei with critical pressures of up to 95.2 kPa below vapour pressure, corresponding to an equivalent bubble diameter of 1.01 μm in the test section.

References

[1] Atlar, M. and Billet, M., Proceedings of the 23rd ITTC Volume II, The specialist committee on water quality and cavitation, 2000.

[2] Brandner, P., Lecoffre, Y. and Walker, G., Design considerations in the development of a modern cavitation tunnel, in *16th Australasian Fluid Mechanics Conf.*, 2007.

[3] Brandner, P., Wright, G., Pearce, B., Goldsworthy, L. and Walker, G., An experimental investigation of microbubble generation in a confined turbulent jet, in *17th Australasian Fluid Mechanics Conf.*, 2010.

[4] Chahine, G. and Shen, Y., Bubble dynamics and cavitation inception in cavitation susceptibility meters, *J. Fluids Eng.*, **108**, 1986, 444–452.

[5] Coleman, H. W. and Steele, W. G., Engineering application of experimental uncertainty analysis, *AIAA journal*, **33**, 1995, 1888–1896.

[6] d'Agostino, L. and Acosta, A., A cavitation susceptibility meter with optical cavitation monitoring part two: experimental apparatus and results, *J. Fluids Eng.*, **113**, 1991, 270–277.

[7] Franc, J.-P. and Michel, J.-M., *Fundamentals of cavitation*, Springer Science & Business Media, 2006.

[8] Gindroz, B. and Billet, M., Influence of the nuclei on the cavitation inception for different types of cavitation on ship propellers, *J. Fluids Eng.*, **120**, 1998, 171–178.

[9] Gowing, S., Comparison of a centerbody and a standard cavitation susceptibility meter, in *ASME/JSME Joint Fluids Eng. Conf., San Francisco, California*, 1999.

[10] Lecoffre, Y., *Cavitation Bubble Trackers*, A. A. Balkema, 1999.

[11] Mées, L., Lebrun, D., Allano, D., Walle, F., Lecoffre, Y., Boucheron, R. and Fréchou, D., Development of interferometric techniques for nuclei size measurement in cavitation tunnel, in *28th Symp. on Naval Hydrodynamics, Pasadena, California*, 2010.

[12] Oldenziel, D., A new instrument in cavitation research: the cavitation susceptibility meter, *J. Fluids Eng.*, **104**, 1982, 136–141.

[13] Pham, T., Michel, J. and Lecoffre, Y., Dynamical nuclei measurement: On the development and the performance evaluation of an optimized center-body meter, *J. Fluids Eng.*, **119**, 1997, 744–751.

[14] Russell, P., Giosio, D., Venning, J., Pearce, B., Brandner, P. and Ceccio, S., Microbubble generation from condensation and turbulent breakup of sheet cavitation, in *31st Symp. on Naval Hydrodynamics, Monterey, California*, 2016.

[15] Shen, Y., Chahine, G., Hsiao, C.-T. and Jessup, S., Effects of model size and free stream nuclei on tip vortex cavitation inception scaling, in *Fourth Int. Symp. on Cavitation, California*, 2001.

[16] Shen, Y. and Gowing, S., Cavitation susceptibility of ocean and laboratory waters, in *21st American Towing Tank Conf., Washington, DC*, 1986.

[17] Venning, J. A., Vincentis, S. D., Pearce, B. W. and Brandner, P. A., Microbubble generation for PIV seeding, in *20th Australasian Fluid Mechanics Conf.*, 2016.